Received: 5 March 2018 | Revised: 27 May 2018 | Accepted: 30 June 2018

DOI: 10.1002/jemt.23101

WILEY MICROSCOPY RESEARCH & TECHNIQUE

RESEARCH ARTICLE

Characterization of ligature-induced experimental periodontitis

Rafael Scaf de Molon[1] | Chan Ho Park[2] | Qiming Jin[3] | Jim Sugai[4] | Joni Augusto Cirelli[1]

[1]Department of Diagnosis and Surgery, School of Dentistry at Araraquara, Sao Paulo State University—UNESP, Araraquara, Brazil

[2]Department of Dental Biomaterials, College of Dentistry, Institute for Biomaterials Research and Development, Kyungpook National University, Daegu, Republic of Korea

[3]Department of Cariology, Restorative Sciences and Endodontics, School of Dentistry, University of Michigan, Ann Arbor, Michigan

[4]Department of Periodontics and Oral Medicine and Center for Craniofacial Regeneration, School of Dentistry, University of Michigan, Ann Arbor, Michigan

Correspondence
Joni Augusto Cirelli, Department of Diagnosis and Surgery, School of Dentistry at Araraquara Sao Paulo State University—UNESP Rua Humaita, 1680, Araraquara, Sao Paulo, 14801-903, Brazil.
Email: cirelli@foar.unesp.br

Abstract

We sought to better characterize the progression of periodontal tissue breakdown in rats induced by a ligature model of experimental periodontal disease (PD). A total of 60 male Sprague–Dawley rats were evenly divided into an untreated control group and a PD group induced by ligature bilaterally around first and second maxillary molars. Animals were sacrificed at 1, 3, 5, 7, 14, and 21 days after the induction of PD. Alveolar bone loss was evaluated by histomorphometry and microcomputed tomography (μCT). The immune-inflammatory process in the periodontal tissue was assessed using descriptive histologic analysis and quantitative polymerase chain reaction (qPCR). This ligature model resulted in significant alveolar bone loss and increased inflammatory process of the periodontal tissues during the initial periods of evaluation (0–14 days). A significant increase in the gene expression of pro-inflammatory cytokines, interleukin-1β (IL-1β), interleukin-6 (IL-6), and tumor necrosis factor-α (TNF-α), and proteins involved in osteoclastogenesis, receptor activator of nuclear factor-k B ligand (RANKL) and osteoprotegerin (OPG) was observed in the first week of analysis. In the later periods of evaluation (14–21 days), no significant alterations were noted with regard to inflammatory processes, bone resorption, and expression of cytokine genes. The ligature-induced PD model resulted in progressive alveolar bone resorption with two different phases: Acute (0–14 days), characterized by inflammation and rapid bone resorption, and chronic (14–21 days) with no significant progression of bone loss. Furthermore, the gene expressions of IL-6, IL-1β, TNF-α, RANKL, and OPG were highly increased during the progress of PD in the early periods.

Research Highlights

- Ligature-induced bone resorption in rats occurred in the initial periods after disease induction
- The bone resorption was characterized by two distinct phases: Acute (0–14 days), with pronounced inflammation and alveolar bone loss
- Chronic phase (14–21 days): No further disease progression
- Several pro-inflammatory cytokines were increased during the progress of periodontitis

KEYWORDS

alveolar bone loss, bone resorption, periodontal disease, periodontitis, rats, X-ray microtomography

1 | INTRODUCTION

Periodontal disease, an infection condition of the supporting tissues around the teeth, is caused by an accumulation of dental biofilm and subsequent release of pro-inflammatory mediators, cytokines, growth factors, and signaling molecules. The persistent presence of oral microorganisms to the dental structures lead to weakened periodontal tissue causing an imbalance in bone metabolism, resulting in substantial alveolar bone resorption (Alencar et al., 2002; de Molon et al., 2016; Mizuno et al., 2015). Recent observations in adult humans identify a prevalence of periodontal disease varying around 46%, which represents 64.7 million people with periodontitis in the U. S. population (Eke et al., 2015), and is considered as the most common cause of tooth loss (Albandar & Rams, 2002).

Uncoupling of bone formation and resorption are associated with a higher degree of tissue breakdown during the course of periodontitis in susceptible hosts. At a histological level, periodontal disease leads to an inflammatory infiltrate composed of neutrophils and leukocytes, which activate immune cells such as lymphocytes to trigger the release of prostaglandins, interleukin-1β (IL-1β), tumor necrosis factor-α (TNF-α), and interleukin-6 (IL-6). These cellular events culminate with the activation of osteoclastogenesis and bone destruction through a direct stimulation of osteoclasts or through the release of tissue-destructive enzymes by the inflammatory cells (Mundy, 1991).

Paralleling clinical observations of periodontal disease, histological and molecular analysis of experimental animal models of periodontitis in mice and rats have provided important insights into the disease pathogenesis recapitulating clinical, radiographic, and histologic features of the disease (de Aquino et al., 2014; de Molon et al., 2014; de Molon, Mascarenhas, et al., 2016; Graves, Fine, Teng, Van Dyke, & Hajishengallis, 2008; Hiyari et al., 2018; Hiyari et al., 2018; Li & Amar, 2007; Polak et al., 2009; Polak, Shapira, Weiss, & Houri-Haddad, 2013; Saadi-Thiers et al., 2013; Wilensky, Gabet, Yumoto, Houri-Haddad, & Shapira, 2005). Moreover, animal models with physiological complications have been extensively utilized to develop new treatment modalities with more effective therapeutic strategies, inquiry host–pathogen interactions, study the effects of surgical interventions, and evaluate the intrinsic effects of periodontal infection or inflammation on systemic conditions (de Molon, de Avila, et al., 2014; de Molon, de Avila, & Cirelli, 2013; de Molon, Mascarenhas, et al., 2016; Graves et al., 2008; Graves, Kang, Andriankaja, Wada, & Rossa Jr., 2012; Matsuda et al., 2015).

Among the various methods employed to mimic periodontitis in animals, the most commonly used model is ligature-induction (de Molon et al., 2013; de Molon, de Avila, et al., 2014; de Molon, Mascarenhas, et al., 2016; Pirih et al., 2015; Wong et al., 2017). The placement of a silk ligature throughout the cervical region of mandibular or maxillary molar teeth leads to bacterial colonization, stimulating a great accumulation of biofilm, resulting in symptoms of disease similar to those observed in a clinical situation, such as apical epithelial migration and bone loss (de Molon, Mascarenhas, et al., 2016; Klausen, 1991; Saadi-Thiers et al., 2013). According to previously published studies in which ligatures are used (Cavagni et al., 2016; de Molon, de Avila, et al., 2014; de Molon, Mascarenhas, et al., 2016; de Souza et al., 2011; Nogueira et al., 2014; Nogueira, de Molon, Nokhbehsaim, Deschner, & Cirelli, 2017), connective tissue and bone loss predictably occurs over a period of 7–15 days in rats and mice. This feature is due to the presence of bacterial species around and within the silk thread, which leads to increased bone destruction in the early stages of disease. A previous report (Bezerra, Brito, Ribeiro, & Rocha, 2002) showed that ligatures did not induce significant bone resorption in germ-free rats and that bacteria accumulation around the thread played an important role in the disease progression (Matsuda et al., 2015). Furthermore, traumatic injury during the pathogenesis of the ligature model has been described in the literature, especially when mouse models are utilized (Abe & Hajishengallis, 2013).

Different data from the literature that directly explore and compare the characteristics of ligature-induced periodontitis during the initial stage of disease are scarce. Here, our aim was to better characterize the ligature-induced periodontal disease model in rats at radiographic microcomputed tomography (μCT), histologic and gene expression of putative pro-inflammatory cytokines in the gingival tissues to more closely investigate periodontitis progression.

2 | MATERIALS AND METHODS

2.1 | Animal care

The experimental protocol (#10343/2010) was handled according to the guidelines of the University of Michigan Institutional Animal Care and Use Committee (IACUC), and all animals received humane care conforms to the animal research: Reporting of in vivo experiments (ARRIVE) guidelines (Kilkenny, Browne, Cuthill, Emerson, & Altman, 2012). Rats were kept in the animal facilities under similar conditions (humidity 60%, temperature-controlled 22 ± 2°C, and 12-hr light/dark cycle). All rats were housed in standard cages in groups of two animals, and water and food were provided ad libitum. A total of 60 2-month-old male Sprague–Dawley rats, with average body weights between 180 and 200 g were randomly, by means of a raffle method, divided into two groups: an untreated control group and a ligature-induced periodontal disease group.

2.2 | Induction of periodontal disease

All animals in the ligature-induced group were anesthetized with an inhalation method using isoflurane (Baxter Healthcare, Deerfield, Illinois) for periodontal disease induction. The ligatures were placed using a sterilized silk thread (Ethicon, Johnson & Johnson, Somerville, New Jersey) tied around the cervix of the first and second maxillary molars in an "8" shape, knotted at the palatal surface of the second molar (Figure 1a–c). To facilitate ligature placement, a slightly separation in the interproximal area between first and second molars with the aid of a periodontal probe (Hu-Friedy, Chicago, Illinois) was performed. In all animals, the ligature was inspected every other day and repositioned if necessary to maintain the ligature during the entire experimental period. Ligatures were maintained in position during the whole experimental period.

2.3 | Maxillae dissection and analyses

At each time point following periodontitis induction, five rats each from the control and experimental group were euthanized per CO_2 overdose. The maxilla from each animal was dissected and then hemisected. One half of each maxilla sample was submitted for alveolar bone level measurements via μCT, after which these were utilized for routine histologic processing for descriptive histological analysis. For the other half maxilla, the gingival tissues around the first and second maxillary molars were gently removed for extraction of total RNA for reverse transcription and quantitative polymerase chain reaction (qPCR). Following gingival tissue dissection, bone samples were immersed in 3% hydrogen peroxide for 24 hr to facilitate the removal of all remaining soft tissue. Samples were then kept in ethanol (70%) until its use for macroscopic evaluation of bone loss.

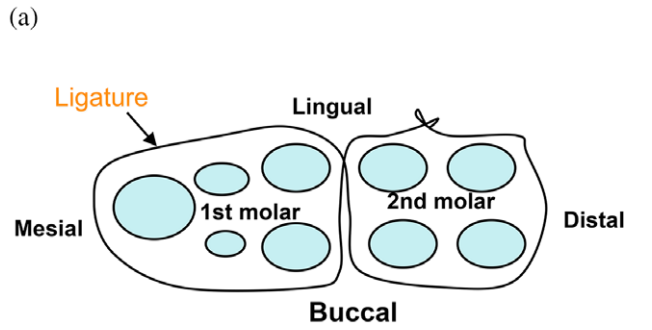

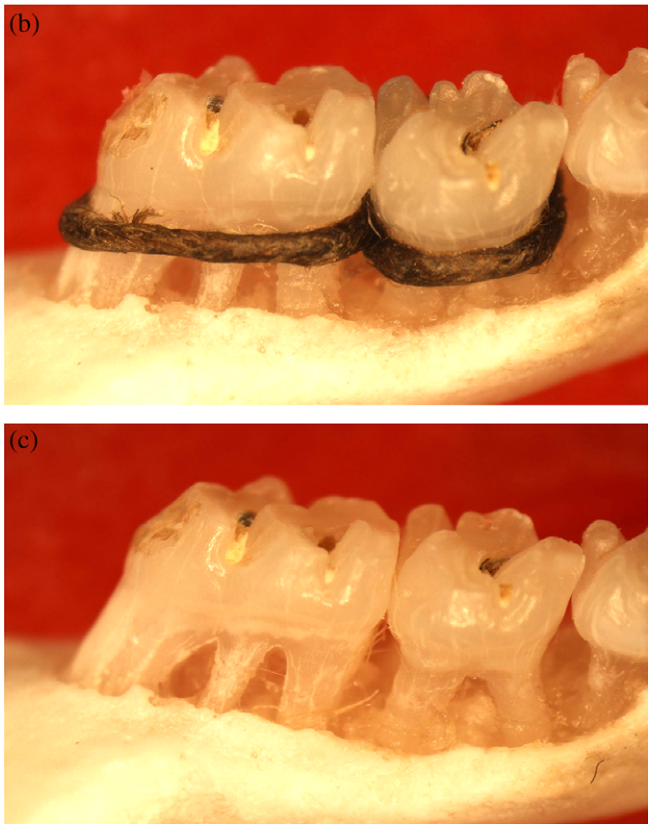

FIGURE 1 (a) Schematic representation of ligature placement around the first and second maxillary molars in an "8" shape and knotted at the palatal surface of the second molar. Ligatures were kept in position during the entire experimental period and were checked every other day and repositioned if necessary. (b–c) Macroscopic views of the molars showing the ligature in placement after (b) soft tissue removal, and the alveolar bone loss induced by the ligature around both molars (c) [Color figure can be viewed at wileyonlinelibrary.com]

2.4 | Macroscopic analysis of bone resorption

The bone resorption area in the buccal and palatal surface of the first and second maxillary molars was macroscopically measured. Briefly, bone samples were removed from the 70% ethanol, dried, submerged for 5 min in methylene blue (0.7 g/L). The samples were then washed with water to eliminate the additional methylene blue stain. Digital photographs of the buccal and palatal surfaces of the stained samples were obtained with a stereomicroscope (Leica Microsystems, Wetzlar, Germany) (20× magnification). The distance from the cemento-enamel junction (CEJ) to the alveolar bone crest (ABC) was measured at six different sites per tooth (mesio-distal, disto-mesial, buccal-palatal, and palatal-buccal regions) and mean values were used. Images from methylene blue-stained samples were measured using appropriate software for 2D-image analysis (Image Pro-Plus 5.1, Rockville, Maryland) by a blinded and calibrated examiner Joni Augusto Cirelli (JAC), as previously described (de Souza et al., 2011). Measurements were performed at baseline, and 7, 14, and 21 days after periodontal disease induction.

2.5 | Microcomputed tomography scanning

Dissected maxillae were carefully harvested, fixed in paraformaldehyde (4%) for 2 days, and stored in ethanol (70%) before μCT scanning. Bone samples were then washed in distilled water and stored in 0.9% saline solution overnight for rehydration. The maxillae were scanned with 18 μm^3 voxel-size by a high-resolution μCT imaging system (GE Healthcare, London, ON, Canada). For sample reconstruction, an analysis software (Microview Analysis+ v.2.1.2, GE Healthcare, Milwaukee, WI, USA) was utilized and the specific parameters used were employed as described elsewhere (Cirelli et al., 2009). The linear bone loss were evaluated by two independent and calibrated examiners, and the measurements were determined from the CEJ to the ABC at the palatal surface of the mesio-palatal and disto-palatal roots of the maxillary first and second molar teeth (Figure 3), as previously described (de Molon et al., 2014; de Molon et al., 2015; de Molon et al., 2016). The linear measurements resulted in an average value, which was used to define the distance from the CEJ to ABC in millimeters.

2.6 | Histologic processing and descriptive analysis

After μCT scanning, the maxilla samples were decalcified in 10% ethylenediaminetetraacetic acid (EDTA), pH 8.0 for 5–6 weeks at room temperature. Samples were paraffin-embedded and 5 μm-thick sections were obtained in the mesio-distal direction. Samples were stained with hematoxylin and eosin (H&E) for histologic descriptive analysis and were evaluated by a blinded and calibrated examiner.

2.7 | Quantitative PCR

Total RNA was extracted from the gingival palatal tissue biopsies collected from the mesial aspect of the first molar to the distal site of the second molar, as previously described (Cirelli et al., 2009). Briefly, RNA purification was achieved using a RNeasy Mini Kit complemented with RNase-free DNase Set (Qiagen, Valencia, California), according to the manufacturer's instructions. Then, a spectrophotometer (BioMate 3, Rochester, New York) was used to measured the purity and quantity of total RNA by evaluating the absorbance at 260 nm and the 260/280 nm ratios, respectively. After the confirmation of the total RNA integrity, cDNA was synthesized by reverse transcription (RT) of 400 ng total RNA in a reverse transcriptase reaction (High capacity cDNA synthesis kit; Applied Biosystems, Foster city, CA, USA), according to the manufacturer protocol.

Real-time qPCR (RT-qPCR) was performed by means of Real Time PCR System (ABI Prism 7,500 StepOne Plus, Applied Biosystems) using TaqMan Gene Expression Assays (Applied Biosystems). The

TABLE 1 Inventoried TaqMan primers and probe

Target gene	ABI ID no	Reporter probe sequence
IL-1β	Rn00580432_m1	CATAAGCCAACAAGTGGTATTCTCC
IL-6	Rn00561420_m1	GAGAAAAGAGTTGTGCAATGGCAAT
TNF-α	Rn99999017_ m1	CACACTCAGATCATCTTCTCAAAAC
RANKL	Rn00589289_m1	TGCCGACATCCCATCGGGTTCCCAT
OPG	Rn00563499_m1	GCTGTGCACTCCTGGTGTTCTTGGA

reaction was performed following the manufacturer's instruction. The determination of the levels of gene expression was performed using the cycle threshold (Ct) method and normalized to the GAPDH (housekeeping gene). The results are represented as the mean ± *SD* mRNA expression from triplicate measurements normalized using the internal control GAPDH, as previously described (Cirelli et al., 2009; de Molon, de Avila, et al., 2014). The target gene, ABI ID no., and reporter probe sequence of each specific TaqMan Gene Expression Assay (Applied Biosystems) are described in Table 1.

2.8 | Statistics

GraphPad Prism Software (La Jolla, California) was used to analyze the raw data. Group measurements were expressed as the mean and standard deviation (SD). Statistical significance was assessed using one-way analysis of variance (ANOVA) followed by the Tukey's post hoc test for multiple comparisons among groups to determine the presence of any significant difference. A significance level of 5% was used.

3 | RESULTS

3.1 | Macroscopic bone resorption analysis

To investigate whether periodontal disease led to bone resorption for the entire experimental period, macroscopic bone loss measurements were performed using methylene blue-stained maxillae samples (Figure 2a–h) at baseline (no ligature) and after 7, 14, and 21 days of periodontitis induction (Figure 2i). Increased bone resorption was predominantly noted after 7 days of disease induction until the 14th day period (Figure 2i). Significant bone resorption was observed from baseline until 14 days after ligature placement in the interproximal area measured in the distal aspect of the first molar ($p < 0.001$) and mesial aspect of the second molar ($p < 0.0001$). After 21 days, statistically significant differences in bone loss were also noted when compared to the baseline and 7-day time points. Interestingly, no significant differences in linear bone loss were found between 14 and 21 days (Figure 2i), which suggests that periodontal disease tends to stabilize during the late periods, characterizing a chronic inflammatory disease.

3.2 | Microcomputed tomography analysis

To further characterize the progression of periodontal disease induced by ligatures, μCT scanning was performed after the end of the experimental periods and linear measurements were made (Figure 3). To quantitate bone loss, the CEJ to ABC distance was

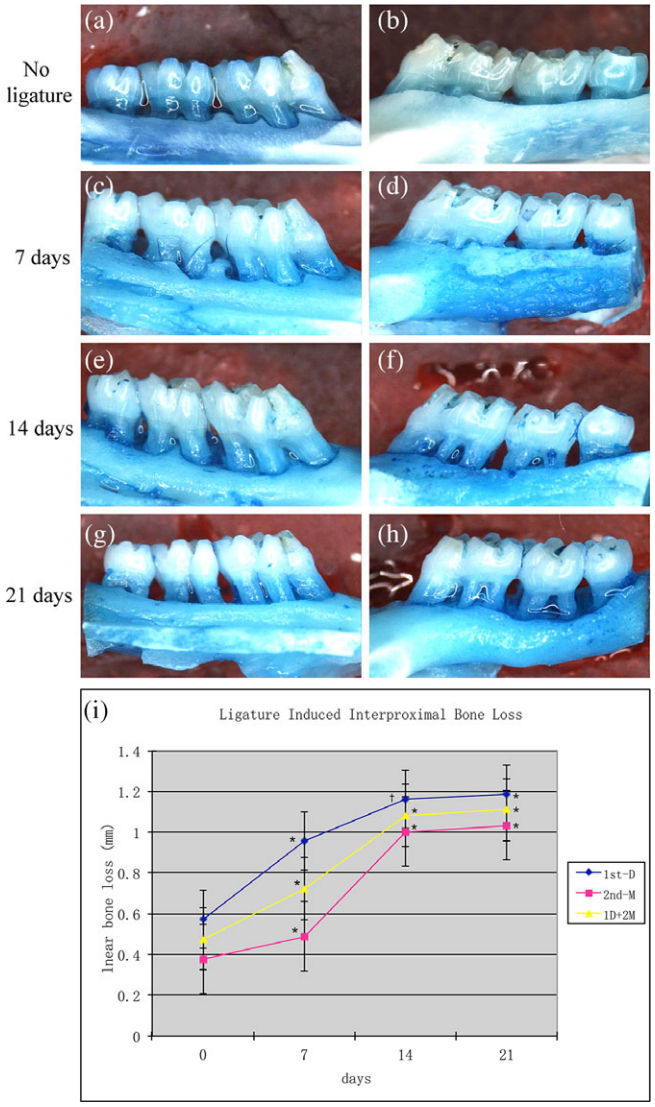

FIGURE 2 (a–d) Representative samples stained with methylene blue in a palatal (a, c, e, g) and buccal (b, d, f, h) view at baseline and after 7, 14, and 21 days of ligature placement. Digital images of the buccal and palatal surfaces of the samples were obtained with a stereomicroscope with 20× magnification. The distance from the CEJ to the ABC was measured at six different sites per tooth (mesio-distal, disto-mesial, buccal-palatal and palatal-buccal regions) and mean values were used. (i) Linear measurements in the distal area of the first molar, mesial aspect of the second molar, and within the interproximal area. Statistically significantly different at $^{\dagger}p < 0.001$, $^{*}p < 0.0001$. Data are represented as mean ±*SD* [Color figure can be viewed at wileyonlinelibrary.com]

measured (Figure 4). No statistically significant differences were found between control and ligature groups at the mesial side of the first molar, throughout the experimental periods (Figure 4a). However, statistically significant differences in bone resorption were found at the distal side of the second molar and within the interproximal area between the first and second molars, 3 days after ligature placement compared to the untreated control group ($p < 0.05$). Progressive bone resorption was evidenced until the 14-day time point, which represents an acute form of the disease (Figure 4d). On the other hand, a slight decrease in bone loss was noted after 15 days of ligature placement, which was sustained until the end of

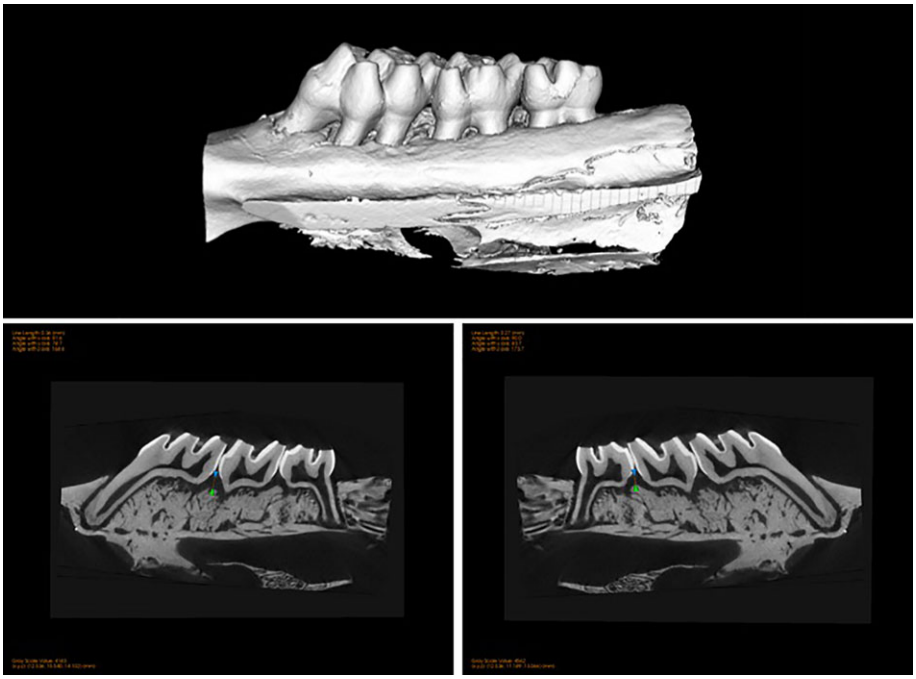

FIGURE 3 Representative 3D images showing the linear measurements performed for each sample. The distance between the CEJ to the ABC was measured in the mesial region of the first molar and distal region of the second molar [Color figure can be viewed at wileyonlinelibrary.com]

the experimental period of 21 days (Figure 4b, c). This situation represents a chronic characteristic of the disease without significant alveolar bone loss progression (Figure 4d). Statistically significant differences in bone loss were evident between the control group and the experimental group until the end of the 21-day period ($p < 0.05$).

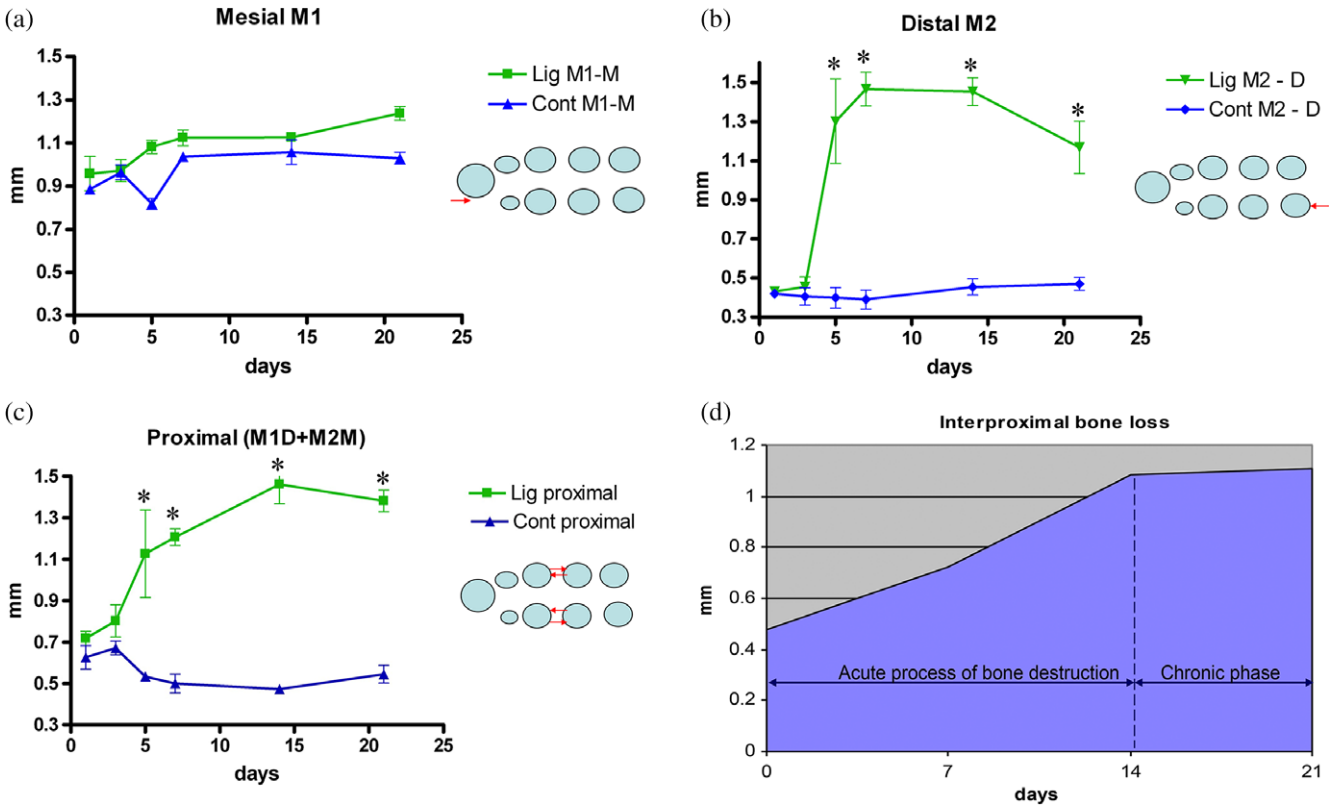

FIGURE 4 Quantification of the μCT linear measurements. Linear bone loss evaluation in the mesial aspect of the first molar (a), distal aspect of the second molar (b) and interproximal area between the first and the second molars (c). The distance from the CEJ to the ABC was measured at the palatal surface of the mesio-palatal and disto-palatal roots of the maxillary first and second molar teeth. Characterization of the two different phases of the disease (d). Statistically significantly different at $^{*}p < 0.05$. Data are represented as mean ± *SD* [Color figure can be viewed at wileyonlinelibrary.com]

3.3 | Histological analysis

To evaluate histologic features of periodontitis, sagittal sections were obtained in the middle of the first and second molar crowns and analysis were performed in the furcation and interproximal area after a period of 1, 3, and 5 days. All untreated control rats showed normal alveolar bone and marginal epithelium, and an absence of inflammatory infiltrate (data not shown). In the experimental group, inflammatory infiltrate (black arrows) was evident 1 day after ligature placement in the furcation and in the interproximal area (Figure 5a–c). Remarkably, bone loss was detected in the ligature group after 1 day of ligature placement represented by an increased distance from the furcation top to the ABC. These findings were maintained 3 and 5 days after disease induction. Collectively, changes in the experimental group included an intense infiltration of inflammatory cells, disrupted epithelial integrity at the dentogingival junction, connective tissue attachment loss, and alveolar bone resorption characterized by an increase in the distance between the CEJ to ABC (Figure 5 a–i).

3.4 | Quantitative PCR

To assess the expression of pro-inflammatory cytokines in the periodontal tissues, qPCR was performed after the end of the experimental period. As expected, significant increases in the mRNA expression

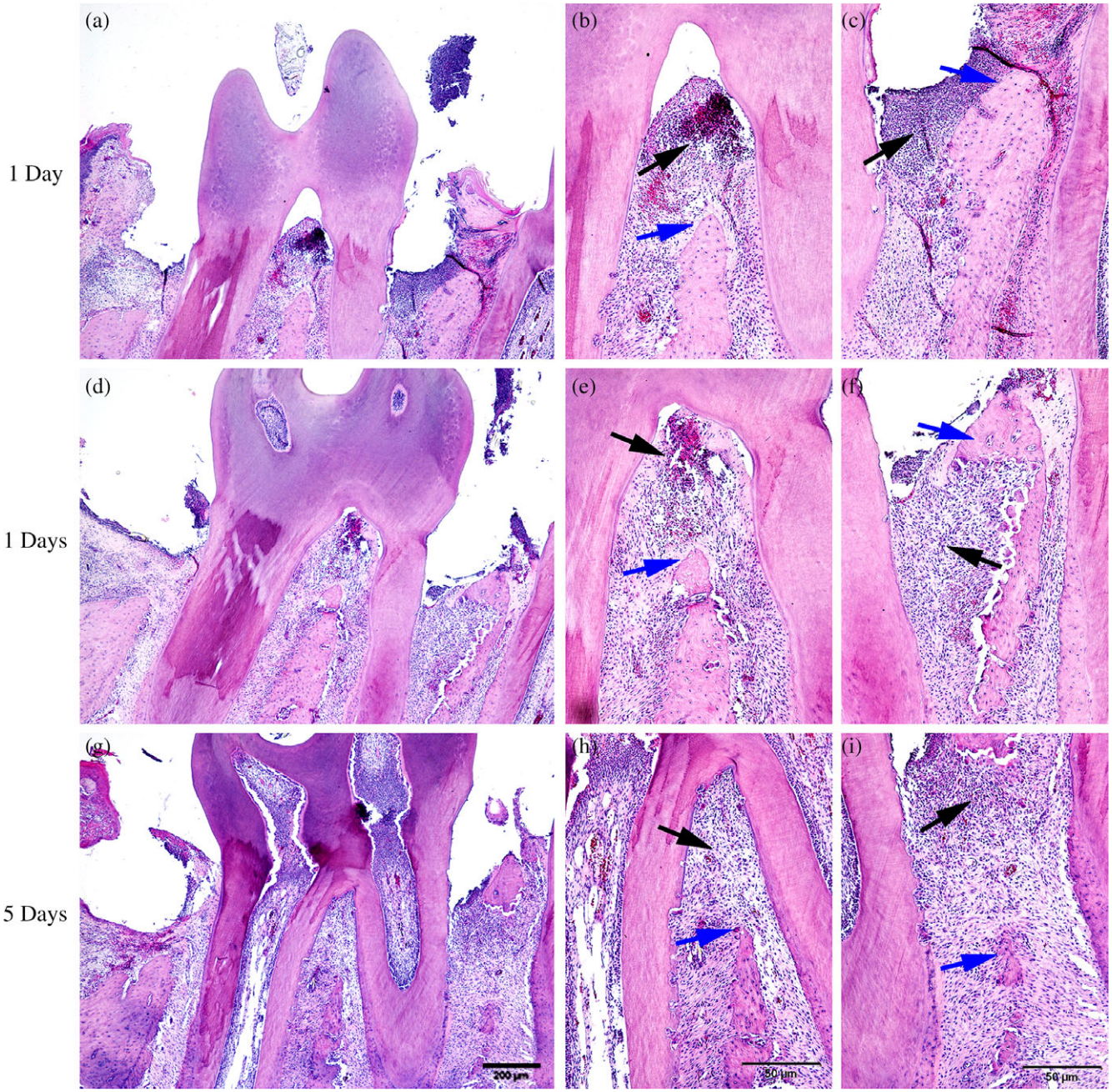

FIGURE 5 Representative histological sections of the experimental groups after periodontitis induction at 1, 3, and 5 days (a, d, g) within the furcation region (b, e, h) and in the interproximal (c, f, i) areas. Samples were paraffin-embedded and 5 µm-thick sections were obtained in the mesio-distal direction and were stained with H&E for descriptive histologic analysis. Black arrows point to inflammatory infiltrate in the connective tissue and the blue arrows point to the alveolar bone crest [Color figure can be viewed at wileyonlinelibrary.com]

of IL-6, IL-1β, and TNF-α were observed during the early periods of the disease; 1 ($p < 0.01$) and 3 ($p < 0.05$) days after ligature placement (Figure 6a, c, e). Accordingly, the mRNA expression of receptor activator of nuclear factor-k B ligand (RANKL), and osteoprotegerin (OPG) was more pronounced in the early periods of the disease (3 and 5 days) with statistically significant differences in the expression of RANKL and OPG after 3 ($p < 0.05$) and 5 days ($p < 0.01$) (Figure 6g–h). After 1 week of disease induction, statistically significant increases in the

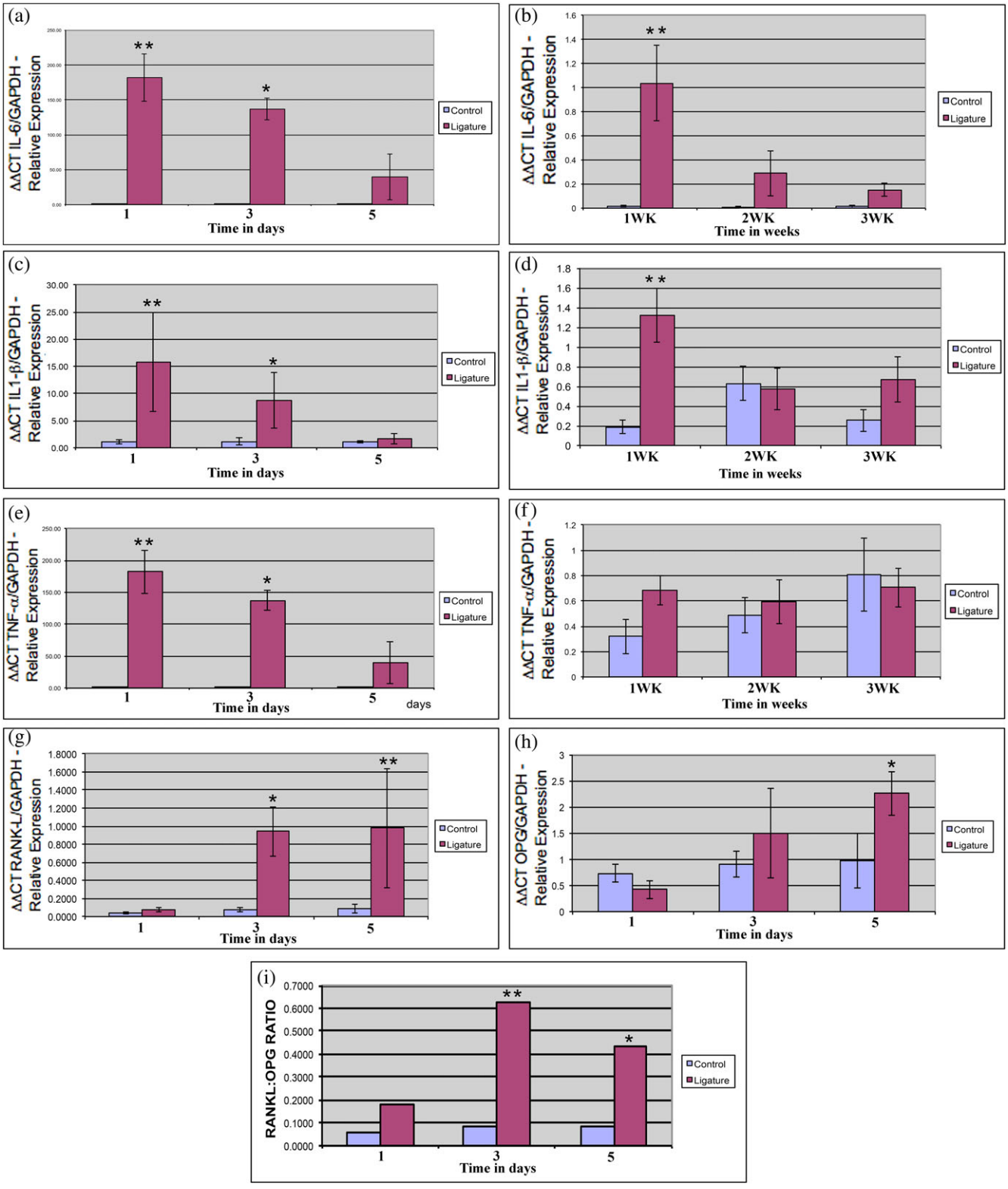

FIGURE 6 qPCR for mRNA expression during the course of the experimental periodontal disease for pro-inflammatory cytokines IL-6 (a, b), IL-1β (c, d), and TNF-α (e, f), and proteins involved in osteoclastogenesis RANKL (g) and OPG (h), and the ratio between RANKL and OPG (i). Gene expression levels were normalized to the housekeeping gene, GAPDH. Statistically significantly different at $^{*}p < 0.05$, $^{**}p < 0.01$. Data are represented as mean ± *SD* [Color figure can be viewed at wileyonlinelibrary.com]

expression of IL-6 and IL-1β were also noted (Figure 6b, d) ($p < 0.01$). No differences were found for TNF-α after 1 week of disease (Figure 6f). In the later periods of evaluation (14–21 days), no statistically significant differences were found for all the cytokines evaluated (Figure 6b, d, f). The ratio of RANKL/OPG was also evaluated and increased ratio in the 3-day period ($p < 0.01$) and 5-day period ($p < 0.05$) after periodontitis induction was observed (Figure 6i).

4 | DISCUSSION

Major progress in the understanding of periodontitis pathogenesis has been made as experimental models of periodontal disease (PD) were first introduced in dental research. However, important gaps in our knowledge still exist related to the ligature-induced periodontitis model. A strategy to overcome these gaps is the extensive effort of research groups to better characterize animal models that closely mimic how periodontitis presents in human beings, assisting in the selection of the most appropriate animal model to be used in preclinical studies according to their objective (de Molon, de Avila, et al., 2014; de Molon, Mascarenhas, et al., 2016; Graves et al., 2008; Graves et al., 2012; Hiyari et al., 2015; Hiyari, Wong, et al., 2018; Li & Amar, 2007; Pirih et al., 2015; Polak et al., 2009; Saadi-Thiers et al., 2013; Wilensky et al., 2005; Wong et al., 2017).

Experimental models for periodontitis in rats and mice have been very beneficial and important to examine various biologic hypotheses in physiological complications and reproduce the radiographic, clinical, molecular, and histologic features of human periodontitis (Anbinder et al., 2016; Cavagni et al., 2016; de Aquino et al., 2014; de Molon, de Avila, et al., 2014; de Molon, Mascarenhas, et al., 2016; Graves et al., 2008; Graves et al., 2012). Animal models of PD allow for studying cellular and molecular mechanisms as well as biological mediators involved during the establishment and progression of the disease and provide valuable information on host–microbial interactions and inflammation (Anbinder et al., 2016; Cavagni et al., 2016; de Aquino et al., 2014; de Molon, de Avila, et al., 2014; de Molon, Mascarenhas, et al., 2016; de Souza et al., 2011; Graves et al., 2008; Matsuda et al., 2015; Mizuno et al., 2015; Nogueira et al., 2014). At this point, ligature-induced PD has been frequently used in periodontal research due to the involvement of live microbes naturally existent in animal species with distinct virulence features, including toxins, pathogen-associated molecular patterns (PAMPs), and products of the microbial metabolism (de Souza et al., 2011). However, the variability of the results found in the literature with regard to this model hinders a definitive conclusion about the true characteristics (initiation and progression) of the disease.

Therefore, using the ligature-induced periodontitis model in rats, we addressed the host response at morphometric, radiographic, histologic, and molecular levels in the beginning stages of the disease through the end of the 21-day experimental period. Our results indicate that the ligature model leads to progressive alveolar bone resorption, suggesting two distinctive phases: (a) an acute phase (0–14 days); (b) a chronic phase (15–21 days). Furthermore, the ligature-induced PD model in an "8" shape placed around the first and second maxillary molars offers a reliable model with site-specific epithelial downgrowth, inflammatory cell infiltration, and time-dependent alveolar bone resorption.

The need to more accurately reflect the clinical reality has led researchers to better characterize the existing animal models (de Molon et al., 2013; de Molon, de Avila, et al., 2014; de Molon, Mascarenhas, et al., 2016; Graves et al., 2008; Graves et al., 2012). In this effort, we used different methodologies to describe the ligature model specifically during the early stages of the disease. Histologic analysis revealed that 1 day after ligature placement, evidence of bone resorption in the furcation and interproximal regions were noted in the ligated animals. The distance from the furcation top to the ABC increased, which denotes increased bone loss. As bone resorption in the ligature model is dependent on the presence of oral microorganisms (Abe & Hajishengallis, 2013; Bezerra et al., 2002; Klausen, 1991; Matsuda et al., 2015), this finding can be attributed to the trauma caused during the ligature placement (Abe & Hajishengallis, 2013). Although μCT analysis had no statistically significant differences in bone resorption within the first 3 days of disease; 5 days after ligature placement, a statistically significant increase in bone resorption was noted radiographically for the experimental group, which increased over time until the 14th day. Importantly, after 14 days of periodontitis, a slight decrease in the amount of bone resorption was evidenced in the interproximal and distal region of the second molar. These results suggest that ligature-induced periodontal disease leads to two distinct phases: an acute phase with progressive destruction of the periodontal tissues (0–14 days) followed by a chronic phase characterized by a cessation of the periodontal inflammation and tissue breakdown. This profile change of ligature-induced bone loss could be potentially explained because, as a consequence of alveolar bone resorption, periodontal tissues tend to migrate to a more apical position to recuperate the biologic space, diminishing the disease severity over time (de Molon, de Avila, et al., 2014; de Molon, Mascarenhas, et al., 2016). However, in this study, the ligature was displayed further apically, every 3 days, to keep the silk thread in close contact with the periodontal tissue, and consequently maintain the inflammation.

In an effort to maintain the disease severity over time, previous studies (Li & Amar, 2007; Saadi-Thiers et al., 2013; Yuan, Gupte, Zelkha, & Amar, 2011) suggest the incubation of live pathogenic microorganisms into the thread, which could lead to an exacerbation of the disease intensity. Microorganisms adhered to the ligature produce several virulence factors, such as PAMPs including some toxins, which might result in a more complex host response, affecting the profile of pro-inflammatory mediators, and periodontal tissue destruction (de Souza et al., 2011). Additionally, a previous study (Anbinder et al., 2016) used ligature placement around the first maxillary molar associated with an oral gavage model using *Porphyromonas gingivalis* to increase the disease severity. Furthermore, the ligature was repositioned apically to sustain the thread in intimate contact with the marginal gingiva. The authors concluded that this model was suitable when advanced bone loss is expected and maintained over time.

Here, mRNA levels of cytokines and other molecules involved in osteoclastogenesis were assessed to determine the inflammatory nature of the disease at a molecular level. The interaction between cytokines and their antagonists will regulate the extent and severity of bone breakdown and tissue destruction mediated by increased

levels of IL-1β, IL-6, TNF-α, and RANKL. We found in the diseased tissues, already at 1 and 3 days of ligature placement that periodontal disease significantly upregulated mRNA expression levels of pro-inflammatory cytokines IL-1β, IL-6, and TNF-α compared to the non-ligated animals. IL-1β and IL-6 levels were also elevated 1 week after disease induction but no differences were found 2 and 3 weeks after periodontitis induction for mRNA expression of the cytokines evaluated.

The binding between RANKL and RANK expressed on osteoclast precursors is the primary event for osteoclasts activation. The effects of RANKL are regulated by OPG that inhibits bone resorption by preventing the interaction of RANK and RANKL (Takayanagi et al., 2002). Alterations in the balance between RANKL and OPG protein expression define the pathogenesis of several metabolic bone diseases, such as periodontitis. In this context, RANKL and OPG expression were significantly higher 3 and 5 days after ligature placement. These findings closely resemble the observations made by previous studies (de Molon, de Avila, et al., 2014; de Souza et al., 2011; Matsuda et al., 2015; Saadi-Thiers et al., 2013) in which increased expression of pro-inflammatory cytokines were noted in the tissue of animals with periodontal disease. The increased microbial burden related with the conversion from health status to periodontal disease might also lead to elevated mRNA expression levels of pro-inflammatory cytokines (de Souza et al., 2011).

An important consideration should be mentioned when interpreting the results of the present investigation. As our focus was mainly in the early stages of disease progression, we evaluated different time points among the analyses. In this regard, histological, radiographic, and gene expression of pro-inflammatory cytokines were investigated in the early phase of disease (after 1, 3, and 5 days). Macroscopic, radiographic, and RT-qPCR analyses were also performed in the late stages of disease progression. Histological analysis was not performed in the late stages of disease because there are already available data characterizing the chronic phase of the disease.

5 | CONCLUSIONS

In summary, our findings in rats provide experimental evidence that ligature-induced periodontal disease offers a consistent model with connective tissue downgrowth, inflammatory cell infiltration, and alveolar bone resorption. Indeed, we showed for the first time that ligature placement could lead to bone resorption within 24 hr, and two distinct phases were characterized when ligatures are used: an acute phase, with progressive inflammation and bone breakdown, followed by a chronic phase, characterized by absence of significant progression of bone loss. Furthermore, the gene expressions of IL-6, IL-1β, TNF-α, RANKL, and OPG were highly increased during the progress of periodontal disease especially in the early periods.

ACKNOWLEDGMENTS

We are extremely grateful to Dr. William V. Giannobile for his help during the experimental design and analysis in this study and for his critical reading of the manuscript.

CONFLICT OF INTEREST

All authors declare that there is no conflict of interest related to this study.

FUNDING INFORMATION

The work was supported by the Department of Periodontics and Oral Medicine and Center for Craniofacial Regeneration, School of Dentistry, University of Michigan.

ORCID

Rafael Scaf de Molon https://orcid.org/0000-0003-1110-6233

REFERENCES

Abe, T., & Hajishengallis, G. (2013). Optimization of the ligature-induced periodontitis model in mice. *Journal of Immunological Methods*, *394*(1–2), 49–54.

Albandar, J. M., & Rams, T. E. (2002). Global epidemiology of periodontal diseases: An overview. *Periodontology 2000*, *29*, 7–10.

Alencar, V. B., Bezerra, M. M., Lima, V., Abreu, A. L., Brito, G. A., Rocha, F. A., & Ribeiro, R. A. (2002). Disodium chlodronate prevents bone resorption in experimental periodontitis in rats. *Journal of Periodontology*, *73*(3), 251–256.

Anbinder, A. L., Moraes, R. M., Lima, G. M., Oliveira, F. E., Campos, D. R., Rossoni, R. D., … Elefteriou, F. (2016). Periodontal disease exacerbates systemic ovariectomy-induced bone loss in mice. *Bone*, *83*, 241–247.

Bezerra, M. M., Brito, G. A., Ribeiro, R. A., & Rocha, F. A. (2002). Low-dose doxycycline prevents inflammatory bone resorption in rats. *Brazilian Journal of Medical and Biological Research*, *35*(5), 613–616.

Cavagni, J., de Macedo, I. C., Gaio, E. J., Souza, A., de Molon, R. S., Cirelli, J. A., … Rosing, C. K. (2016). Obesity and hyperlipidemia modulate alveolar bone loss in Wistar rats. *Journal of Periodontology*, *87*(2), e9–e17.

Cirelli, J. A., Park, C. H., MacKool, K., Taba, M., Jr., Lustig, K. H., Burstein, H., & Giannobile, W. V. (2009). AAV2/1-TNFR:Fc gene delivery prevents periodontal disease progression. *Gene Therapy*, *16*(3), 426–436.

de Aquino, S. G., Abdollahi-Roodsaz, S., Koenders, M. I., van de Loo, F. A., Pruijn, G. J., Marijnissen, R. J., … van den Berg, W. B. (2014). Periodontal pathogens directly promote autoimmune experimental arthritis by inducing a TLR2- and IL-1-driven Th17 response. *Journal of Immunology*, *192*(9), 4103–4111.

de Molon, R. S., Cheong, S., Bezouglaia, O., Dry, S. M., Pirih, F., Cirelli, J. A., … Tetradis, S. (2014). Spontaneous osteonecrosis of the jaws in the maxilla of mice on antiresorptive treatment: A novel ONJ mouse model. *Bone*, *68*, 11–19.

de Molon, R. S., de Avila, E. D., Boas Nogueira, A. V., Chaves de Souza, J. A., Avila-Campos, M. J., de Andrade, C. R., & Cirelli, J. A. (2014). Evaluation of the host response in various models of induced periodontal disease in mice. *Journal of Periodontology*, *85*(3), 465–477.

de Molon, R. S., de Avila, E. D., & Cirelli, J. A. (2013). Host responses induced by different animal models of periodontal disease: A literature review. *Journal of Investigative and Clinical Dentistry*, *4*(4), 211–218.

de Molon, R. S., Hsu, C., Bezouglaia, O., Dry, S. M., Pirih, F. Q., Soundia, A., … Tetradis, S. (2016). Rheumatoid arthritis exacerbates the severity of osteonecrosis of the jaws (ONJ) in mice. A randomized, prospective, controlled animal study. *Journal of Bone and Mineral Research*, *31*(8), 1596–1607.

de Molon, R. S., Mascarenhas, V. I., de Avila, E. D., Finoti, L. S., Toffoli, G. B., Spolidorio, D. M., … Cirelli, J. A. (2016). Long-term evaluation of oral gavage with periodontopathogens or ligature induction of experimental periodontal disease in mice. *Clinical Oral Investigations*, *20*(6), 1203–1216.

de Molon, R. S., Shimamoto, H., Bezouglaia, O., Pirih, F. Q., Dry, S. M., Kostenuik, P., … Tetradis, S. (2015). OPG-Fc but not Zoledronic acid

discontinuation reverses osteonecrosis of the jaws (ONJ) in mice. *Journal of Bone and Mineral Research*, *30*(9), 1627–1640.

de Souza, J. A., Nogueira, A. V., de Souza, P. P., Cirelli, J. A., Garlet, G. P., & Rossa, C., Jr. (2011). Expression of suppressor of cytokine signaling 1 and 3 in ligature-induced periodontitis in rats. *Archives of Oral Biology*, *56*(10), 1120–1128.

Eke, P. I., Dye, B. A., Wei, L., Slade, G. D., Thornton-Evans, G. O., Borgnakke, W. S., … Genco, R. J. (2015). Update on prevalence of periodontitis in adults in the United States: NHANES 2009 to 2012. *Journal of Periodontology*, *86*(5), 611–622.

Graves, D. T., Fine, D., Teng, Y. T., Van Dyke, T. E., & Hajishengallis, G. (2008). The use of rodent models to investigate host-bacteria interactions related to periodontal diseases. *Journal of Clinical Periodontology*, *35*(2), 89–105.

Graves, D. T., Kang, J., Andriankaja, O., Wada, K., & Rossa, C., Jr. (2012). Animal models to study host-bacteria interactions involved in periodontitis. *Frontiers of Oral Biology*, *15*, 117–132.

Hiyari, S., Atti, E., Camargo, P. M., Eskin, E., Lusis, A. J., Tetradis, S., & Pirih, F. Q. (2015). Heritability of periodontal bone loss in mice. *Journal of Periodontal Research*, *50*(6), 730–736.

Hiyari, S., Naghibi, A., Wong, R., Sadreshkevary, R., Yi-Ling, L., Tetradis, S., … Pirih, F. Q. (2018). Susceptibility of different mouse strains to peri-implantitis. *Journal of Periodontal Research*, *53*(1), 107–116.

Hiyari, S., Wong, R. L., Yaghsezian, A., Naghibi, A., Tetradis, S., Camargo, P. M., & Pirih, F. Q. (2018). Ligature-induced peri-implantitis and periodontitis in mice. *Journal of Clinical Periodontology*, *45*(1), 89–99.

Kilkenny, C., Browne, W. J., Cuthill, I. C., Emerson, M., & Altman, D. G. (2012). Improving bioscience research reporting: The ARRIVE guidelines for reporting animal research. *Osteoarthritis and Cartilage*, *20*(4), 256–260.

Klausen, B. (1991). Microbiological and immunological aspects of experimental periodontal disease in rats: A review article. *Journal of Periodontology*, *62*(1), 59–73.

Li, C. H., & Amar, S. (2007). Morphometric, histomorphometric, and microcomputed tomographic analysis of periodontal inflammatory lesions in a murine model. *Journal of Periodontology*, *78*(6), 1120–1128.

Matsuda, Y., Kato, T., Takahashi, N., Nakajima, M., Arimatsu, K., Minagawa, T., … Yamazaki, K. (2015). Ligature-induced periodontitis in mice induces elevated levels of circulating interleukin-6 but shows only weak effects on adipose and liver tissues. *Journal of Periodontal Research*, *5*(51), 639–646.

Mizuno, M., Miyazawa, K., Tabuchi, M., Tanaka, M., Yoshizako, M., Minamoto, C., … Goto, S. (2015). Reveromycin a administration prevents alveolar bone loss in Osteoprotegerin knockout mice with periodontal disease. *Scientific Reports*, *5*, 16510.

Mundy, G. R. (1991). Inflammatory mediators and the destruction of bone. *Journal of Periodontal Research*, *26*(3 Pt 2), 213–217.

Nogueira, A. V., de Molon, R. S., Nokhbehsaim, M., Deschner, J., & Cirelli, J. A. (2017). Contribution of biomechanical forces to inflammation-induced bone resorption. *Journal of Clinical Periodontology*, *44*(1), 31–41.

Nogueira, A. V., de Souza, J. A., de Molon, R. S., Pereira Eda, S., de Aquino, S. G., Giannobile, W. V., & Cirelli, J. A. (2014). HMGB1 localization during experimental periodontitis. *Mediators of Inflammation*, *2014*, 1–10.

Pirih, F. Q., Hiyari, S., Barroso, A. D., Jorge, A. C., Perussolo, J., Atti, E., … Camargo, P. M. (2015). Ligature-induced peri-implantitis in mice. *Journal of Periodontal Research*, *50*(4), 519–524.

Polak, D., Shapira, L., Weiss, E. I., & Houri-Haddad, Y. (2013). Virulence mechanism of bacteria in mixed infection: Attenuation of cytokine levels and evasion of polymorphonuclear leukocyte phagocytosis. *Journal of Periodontology*, *84*(10), 1463–1468.

Polak, D., Wilensky, A., Shapira, L., Halabi, A., Goldstein, D., Weiss, E. I., & Houri-Haddad, Y. (2009). Mouse model of experimental periodontitis induced by *Porphyromonas gingivalis/Fusobacterium nucleatum* infection: Bone loss and host response. *Journal of Clinical Periodontology*, *36*(5), 406–410.

Saadi-Thiers, K., Huck, O., Simonis, P., Tilly, P., Fabre, J. E., Tenenbaum, H., & Davideau, J. L. (2013). Periodontal and systemic responses in various mice models of experimental periodontitis: Respective roles of inflammation duration and *Porphyromonas gingivalis* infection. *Journal of Periodontology*, *84*(3), 396–406.

Takayanagi, H., Kim, S., Matsuo, K., Suzuki, H., Suzuki, T., Sato, K., … Taniguchi, T. (2002). RANKL maintains bone homeostasis through c-Fos-dependent induction of interferon-beta. *Nature*, *416*(6882), 744–749.

Wilensky, A., Gabet, Y., Yumoto, H., Houri-Haddad, Y., & Shapira, L. (2005). Three-dimensional quantification of alveolar bone loss in *Porphyromonas gingivalis*-infected mice using micro-computed tomography. *Journal of Periodontology*, *76*(8), 1282–1286.

Wong, R. L., Hiyari, S., Yaghsezian, A., Davar, M., Lin, Y. L., Galvan, M., … Pirih, F. Q. (2017). Comparing the healing potential of late-stage periodontitis and peri-implantitis. *The Journal of Oral Implantology*, *43*(6), 437–445.

Yuan, H., Gupte, R., Zelkha, S., & Amar, S. (2011). Receptor activator of nuclear factor kappa B ligand antagonists inhibit tissue inflammation and bone loss in experimental periodontitis. *Journal of Clinical Periodontology*, *38*(11), 1029–1036.

How to cite this article: de Molon RS, Park CH, Jin Q, Sugai J, Cirelli JA. Characterization of ligature-induced experimental periodontitis. *Microsc Res Tech*. 2018;81:1412–1421. https://doi.org/10.1002/jemt.23101